Acoustic Radiation Force: A Review of Four Mechanisms for Biomedical Applications

Armen P. Sarvazyan, Oleg V. Rudenko, and Mostafa Fatemi, *Life Fellow, IEEE*

***Abstract*—Radiation force is a universal phenomenon in any wave motion where the wave energy produces a static or transient force on the propagation medium. The theory of acoustic radiation force (ARF) dates back to the early 19th century. In recent years, there has been an increasing interest in the biomedical applications of ARF. Following a brief history of ARF, this article describes a concise theory of ARF under four physical mechanisms of radiation force generation in tissue-like media. These mechanisms are primarily based on the dissipation of acoustic energy of propagating waves, the reflection of the incident wave, gradients of the compressional wave speeds, and the spatial variations of energy density in standing acoustic waves. Examples describing some of the practical applications of ARF under each mechanism are presented. This article concludes with a discussion on selected ideas for potential future applications of ARF in biomedicine.**

***Index Terms*—Acoustics, biomedicine, imaging, radiation force, ultrasound.**

Nomenclature

a	Initial beam radius.
c	Sound velocity.
dV	Infinitesimal volume element.
$\vec{f} = f_i = (f_x, f_y, f_z)$	Radiation force acting on a unit volume of the medium.
$\vec{F} = F_i = (F_x, F_y, F_z)$	Radiation force acting on a body of finite size.
G	Shear modulus.
K	Bulk compression modulus.
k_n	Wavenumber for the nth mode.
$\vec{n} = n_i$	Unit normal vector to the surface S.
p	Acoustic pressure.
$P_0(t)$	Envelope of pulse.
P_0	Amplitude of pressure wave.
r	Radial coordinate.
R	Distance from the sound source to the focus.
S	Surface surrounding the selected volume V.
u_i	Particle velocity vector components.
$\vec{U}$	Displacement of medium element vector.
V	Volume.
W	Potential energy.
x	Longitudinal coordinate.
α	Damping coefficient.
γ	Form factor (a number).
κ	Refection coefficient.
ρ	Medium density.
ω	Angular frequency
σ_{ik}	Stress tensor.
$\langle \cdots \rangle$	Brackets mean averaging over the oscillation period.
∇	Gradient operator.
Δ	Laplace operator.
sin	Trigonometry function (sine).
exp	Exponential function.
$\int$	Integral.
$\oint$	Closed surface integral.

Manuscript received June 26, 2021; accepted September 9, 2021. Date of publication September 14, 2021; date of current version October 22, 2021. *(Corresponding author: Mostafa Fatemi.)*

Armen P. Sarvazyan is with Artann Laboratories, Lambertville, NJ 08530 USA (e-mail: armen@artannlabs.com).

Oleg V. Rudenko is with the Department of Acoustics, Moscow State University, 119991 Moscow, Russia, also with the Prokhorov Institute of General Physics, Russian Academy of Sciences, 119991 Moscow, Russia, and also with the Institute of the Physics of the Earth, Russian Academy of Sciences, 123995 Moscow, Russia (e-mail: rudenko@acs366.phys.msu.ru).

Mostafa Fatemi is with the Department of Physiology and Biomedical Engineering, Mayo Clinic College of Medicine and Science, Rochester, MN 55905 USA (e-mail: fatemi.mostafa@mayo.edu).

Digital Object Identifier 10.1109/TUFFC.2021.3112505

I. Introduction and Brief History

RADIATION force is a universal phenomenon in any type of wave motion. Acoustic waves produce different types of radiation force caused by a change in the density of energy and momentum of the propagating wave. The history of acoustic radiation force (ARF) is in detail described in our review article "Biomedical applications of radiation force of ultrasound: Historical roots and physical basis" [1]. First observations of radiation force were made by Faraday [2], and Kundt and Lehmann [3], and the physics of ARF was first analyzed by Rayleigh [4]. Further progress in ARF studies in the following decades was made in experimental works by Bjerknes [5], Wood and Loomis [6], and Hertz and Mende [7]. In the following decades, Leon Brillouin

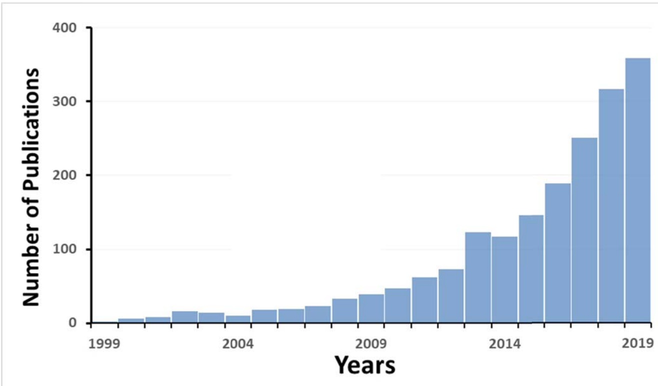

Fig. 1. Dynamics of publications on ARF-based SWE.

and Paul Langevin (1932) made significant progress in the theory of radiation force [8]. Closer to the end of the century, numerous biomedical applications of ARF were developed and the biophysical basis of these applications was presented in reviews and original articles of Nyborg [9] and [10]. Newly developed areas of biomedical applications of ARF included ARF Impulse Imaging, Vibro-acoustography, shear wave elasticity imaging (SWEI), SuperSonic Shear Imaging, Harmonic Motion Imaging, MR elastography, assessment of biological fluids' and tissues' viscoelastic properties, monitoring lesions during therapy, assisting targeted drug and gene delivery, and manipulation of biological cells and particles in standing ultrasonic wave fields [1], [11]–[24].

Currently, the widest area of biomedical applications of radiation force is related to medical imaging [11]–[13], [24] and, more specifically, to shear wave elastography (SWE) [25]. The radiation force of a focused ultrasound beam acts as a virtual finger for remote probing internal tissue structures and obtaining diagnostic information. Fig. 1 illustrates the dynamics of publications on ARF-based SWE according to the PubMed database for the last two decades (1999–2019). This type of exponential growth is typical for publications on many biomedical applications of ARF.

A list of variables, function, and operations used in this article and their dentitions are provided in Nomenclature.

II. Physical Mechanisms of Generation of Radiation Force in Tissue-Like Media

Mechanisms of ARF generation include [11] the following.

(A) Change in the density of energy of the propagating wave due to dissipation of energy because of absorption and scattering.

(B) Reflection from various types of interfaces, such as inclusions, walls, or other interfaces.

(C) Spatial variations of energy density in standing acoustic waves.

(D) Spatial variations in propagation velocity and/or density of the medium.

In Sections II-A–II-D, we describe each mechanism with some representative examples of its biomedical applications.

A. Mechanism a

Let us refer to ARF produced by the mechanism (A) as A-ARF.

The A-ARF, which is based on the dissipation of acoustic energy of propagating waves, is one of the most widely used acoustic techniques in medical imaging.

This loss of acoustic energy responsible for A-ARF may happen due to wave dissipation, which means the transformation of mechanical energy into heat. In this case, the mechanical moment of the wave is partly transferred to the absorbing medium and it creates a radiation force. Losses can also occur due to the scattering when the part of energy carried by the wave begins to flow at different angles to the original direction of propagation of the wave. Strictly speaking, scattering in a medium does not lead to dissipation of the wave, but to decrease in its amplitude.

Let the radiation force acting on a unit volume of the medium be $\vec{f} = f_i = (f_x, f_y, f_z)$. A force $f_i dV$ acts on a small volume dV. To calculate the radiation force for a body of finite size, it is necessary to integrate over the volume or over the closed body surface (S) [26]

$$F_i = \int f_i dV = \int \frac{\partial \sigma_{ik}}{\partial x_k} dV = \oint \sigma_{ik} n_k dS. \quad (1)$$

Here, as it is customary in the theory of elasticity, tensor notation is used. The summation is performed over twice repeating indices, that is $\sigma_{ik} n_k = \sigma_{i1} n_1 + \sigma_{i2} n_2 + \sigma_{i3} n_3 = \sigma_{ix} n_x + \sigma_{iy} n_y + \sigma_{iz} n_z$. Here $\vec{n} = n_i$ is the unit normal vector to the surface S surrounding the selected volume V, and σ_{ik} is the stress tensor. Expression (1) is commonly used in the theory of elasticity. It is written in the Lagrange representation.

The propagation of acoustic waves in soft tissues can usually be described by equations of fluid mechanics, and in formula (1) one should put $\sigma_{ik} = -p\delta_{ik} + \rho u_i u_k$ [27]. Here u_i is the particle velocity, p is pressure, and ρ is the medium density. When describing the fluid, it is customary to use Euler's approach [28].

Radiation forces in solids depend on spatial derivatives of the displacement vector. Forces contain both linear and non-linear combinations of these derivatives. Therefore

$$\vec{F} = \vec{F}^{\mathrm{LIN}} + \vec{F}^{\mathrm{NL}}. \quad (2)$$

For linear combination, as it is well known, $\vec{f}^{\mathrm{LIN}} = (K + G/3)\nabla\nabla\vec{U} + G\Delta\vec{U}$, where $\vec{U}$ is the displacement vector. The nonlinear part is cumbersome and is not specified here. K is the bulk compression modulus, and G is the shear modulus.

If the periodic oscillations contain several harmonics like in sawtooth wave

$$\left\langle \vec{F}^{\mathrm{LIN}} \right\rangle = 0, \quad \left\langle \vec{F} \right\rangle = \left\langle \vec{F}^{\mathrm{NL}} \right\rangle. \quad (3)$$

Here, the angle brackets mean averaging over the oscillation period. The radiation force is completely determined by nonlinear terms.

It should be noted that nonlinearity in solids could be of a different nature. The nonlinear term in the relationship between stress and strain tensors is referred to as "geometric" nonlinearity. The nonlinearity of Hooke's law, usually written in terms of Landau moduli, is called "physical." The third type is huge "structural" nonlinearity; it occurs in defected and granular media as well as in condensed media saturated with gas bubbles. The fourth type (boundary nonlinearity) is associated with finite displacements of an oscillating source. These nonlinearities and corresponding phenomena are reviewed in [29] and [30].

Complete expressions for the radiation force with allowance for geometric and physical nonlinearities are given, for example, in [30]. They are very cumbersome, and, therefore, are not presented here.

For the sake of simplicity and demonstration of the basic ideas, we restrict ourselves to the approximations made in [31]. This gives the formula

$$\left\langle \vec{f}^{\mathrm{NL}} \right\rangle = -\frac{1}{c^2\rho}\nabla\left\langle p^2\right\rangle. \tag{4}$$

Here $\mathcal{C}$ is the sound velocity.

It is helpful to emphasize the analogy between (4) and the general relationship $\vec{F} = -\nabla W$ between force and potential energy W. One can see that $\langle p^2\rangle/c^2\rho$ plays the role of a potential function.

For a plane monochromatic wave attenuating due to dissipative or scattering properties of the medium, we obtain

$$p = P_0 \exp(-\alpha x)\sin\omega\left(t - \frac{x}{c}\right)$$
$$\left\langle f_x^{NL}\right\rangle = \frac{\alpha P_0^2}{c^2\rho}\exp(-2\alpha x). \tag{5}$$

Due to attenuation, a dependence on the longitudinal coordinate x exists in the averaged expression for $\langle p^2\rangle$. Because of this, when differentiating (4), a nonzero force appears along the direction of wave propagation that is proportional to the damping coefficient α. This is typical A-ARF. It should be noted that if the amplitude depends on the transverse coordinates, the plane wave turns into a wave beam. In this case, "transverse" components f_y^{NL}, f_z^{NL} of the radiation force will also appear.

1) Biomedical Applications: Examples of A-ARF-based modalities are SWEI [24], [25] and ARF Impulse Imaging [12], [13] developed in the 1990s. There are two synonyms: "Elasticity Imaging" and "Elastography" used in describing these A-ARF-based technologies. The first ultrasonic elastographic technology that uses ARF-generated shear waves is SWEI, more often called SWE, not SWEI, apparently renaming the original technology. Numerous other elastographic modalities using A-ARF were developed in the next decade. These modalities include but are not limited to SuperSonic Imaging [32], Harmonic Motion Imaging [33], crawling wave estimator [34], shearwave dispersion ultrasound vibrometry (SDUV) [35], lamb wave dispersion ultrasound vibrometry (LDUV) [36], attenuation measuring ultrasound shear wave elastography (AMUSE) [37], ARF Induced Creep-Recovery [38], Local Phase Velocity-Based Imaging [39], viscoelastic response (VisR) Imaging [40], Shear Wave Spectroscopy for quantification of tissue viscoelasticity [41], fractional derivative group shear estimation [42], reverberant shear wave fields for estimation of shear wave speed [43], two-point frequency shift for shear wave attenuation measurement [44], and spatially-modulated ultrasound radiation force (STL-SWE/SMURF) [45]. A detailed description of the clinical applications of selected technologies based on mechanism A-ARF can be found in [12] and [24]. To date, numerous review articles have been published on ARFI, SWE, and SuperSonic Imaging. A more recent review of these elastography techniques and their clinical applications can be found in [46]. SWE has found clinical success in staging liver fibrosis, and in the visualization of soft tissue lesions in the breast, thyroid, and prostate [47]–[51].

An example of non-imaging application of A-ARF is in the investigation of the mechanical properties of the urinary bladder. The overall approach is based on the ARF-induced Lamb waves in the bladder wall to evaluate the detrusor muscle compliance in the neurogenic bladders [52]–[54]. Another example where A-ARF has been used to exploit guided waves phenomena is to measure the stiffness of arterial walls [55], [56]. Vibro-acoustography is another imaging technique that benefits from the A-ARF mechanism [57]–[59] where tissue attenuation is the main contributor to the generation of ARF.

B. Mechanism B

Radiation force based on mechanism (B), let it be called B-ARF, arises from the reflection of the incident wave from various interfaces. The B-ARF is the basis of radiation force balance, one of the earliest applications of ARF, to measure the total power in ultrasonic beams for testing ultrasonic therapy devices [6]. In the simplest case, B-ARF occurs when a wave is reflected from an immovable wall.

Let us use the expression following from formulas (1) and (4):

$$F_i^{\mathrm{NL}} = \int \langle f_i^{\mathrm{NL}}\rangle dV = -\frac{1}{c^2\rho}\oint \langle p^2\rangle n_i dS. \tag{6}$$

For the incident and reflected plane harmonic waves traveling along x, we have

$$p^{\mathrm{IN}} = P_0 \sin\left(t - \frac{x}{c}\right)$$
$$p^{\mathrm{REF}} = \kappa P_0 \sin\left(t + \frac{x}{c}\right)$$
$$\left\langle p^2\right\rangle\Big|_{x=0} = \frac{(1+\kappa)^2}{2}P_0^2. \tag{7}$$

Here κ is the coefficient of reflection from the wall. If $\kappa = 1$, we get an ideal reflection, which is similar to an elastic ball-wall collision. In this case, the double moment of the ball transmits to the wall.

Let us take into account that the acoustic field exists only in front of the wall, but not behind the wall. In this situation, formulas (6) yield

$$F_x^{\mathrm{NL}} = \frac{(1+\kappa)^2}{2c^2\rho}P_0^2 S. \tag{8}$$

So, reflecting from a rigid fixed boundary, the wave pushes it forward. For brevity, we do not discuss the difference between Rayleigh and Langevin radiation pressures, i.e., two types of radiation force analyzed in detail in numerous theoretical studies [60]–[62].

Another type of B-ARF appears when an acoustic wave reflects from a solid particle or other reflecting inhomogeneity. Now the problem becomes 3-D and requires the use of complex formulas describing a wave scattered in all directions on a specific irregularity. It is convenient to calculate the reaction force from the scattered field in the far zone, where the wave becomes spherically divergent. In this case, the expression of the following form should be substituted into Formula (6):

$$\langle p^2 \rangle = \frac{1}{2} P_0^2 \left(\frac{r_0}{r}\right)^2 A^2(\theta, \phi). \tag{9}$$

Here θ, ϕ are the polar and azimuthal angles of the spherical coordinate system. The polar axis is aligned with the $\mathcal{X}$-direction. The function $A(\theta, \phi)$ determines the angular distribution of the amplitude or the directivity characteristic of the scattering. There are many single and multiple scatterers with different shapes, density, and compressibility. Due to the great variety of scatterers, for each of them, the function $A(\theta, \phi)$ has its own specific form, we refer to the general theory of sound scattering by inhomogeneities described in the textbook [26], paragraph 58. As examples, two specific functions are given in [26], the first for the scattering cross-section of a plane wave on a solid ball, and the second for the scattering on a liquid drop, taking into account its radial and translational vibration caused by an acoustic wave.

1) Biomedical Applications: This mechanism is the basis of many applications employing vibro-acoustography principles developed by Fatemi, Greenleaf, and their coworkers [57], [59], [63]. In such applications, tissue reflection is considered the main contributor to the generation of ARF. The clinical applications of vibro-acoustography for breast imaging can be found in [64]–[66]. Applications of vibro-acoustography for other organs, such as thyroid [67], prostate [68]–[70], kidney [71], and peripheral arteries [72] have been reported. Review articles on vibro-acoustography and its potential applications in medicine are presented in [58], and more recently in [73]. The B-ARF mechanism is also used to reposition kidney stones and improve the clearance of residual stone fragments after surgical management [74].

C. Mechanism C

The ARF based on mechanism (C), let it be called C-ARF, results from the spatial variations of energy density in standing acoustic waves.

By description, the acoustic pressure in a standing wave is $p = P_0 \sin(\omega t) \cos(k_n x)$, where k_n are the wave numbers for different modes determined by the boundary conditions. The density of the radiation force has the following 1-D structure:

$$\langle f_x^{\mathrm{NL}} \rangle = \frac{k_n P_0^2}{2c^2 \rho} \sin(2k_n x). \tag{10}$$

The force (10) tends to "push" the particles out of the antinodes and concentrate them at the nodes of the standing wave, or acts in the opposite direction. In particular, spherical balls with a density greater than the density of the liquid move to the antinodes of the vibrational speed, and if the density of the particle material is low, they tend to concentrate at the speed nodes. Bunching of particles was observed for the first time in classical experiments in the Kundt tube.

Manipulating particles with a standing wave is similar to another manipulation method—using transverse field gradients in an acoustic beam. The bulk density of the radiation force for a circular in cross-section Gaussian beam was calculated in [75]

$$\langle \vec{f}^{\mathrm{NL}} \rangle = -\frac{P_0^2}{2c^2 \rho} \nabla \frac{1}{g^2} \exp\left(-\frac{2r^2}{a^2 g^2}\right)$$
$$g(x) = \sqrt{\left(1 - \frac{x}{R}\right)^2 + \frac{x^2}{x_{\mathrm{DIF}}^2}}. \tag{11}$$

Here R is the distance from the sound source to the focus, $x_{\mathrm{DIF}} = \omega a^2/2c$ is the diffraction length, and a is the initial beam radius. According to the first formula (11), the radial component of the radiation force is calculated by replacing the gradient operator by differentiation with respect to r. We see that the radial component depends on the radial coordinate r as $r \exp(-r^2/a^2)$. Consequently, the radiation force is directed from the beam axis.

If there is a particle in the beam, it can be pushed out from the beam axis or, on the contrary, be attracted to the center, depending on its properties. One can create a beam that has a dip on the axis. In this case, the force will change its direction. This beam can be used in tweezers to capture and manipulate particles in the liquid.

1) Biomedical Applications: The C-ARF has been extensively studied in the last couple of decades [15]–[23]. It has been employed for manipulating (separating, washing, sorting, and isolating) biological cells and particles as well as for enhancing bead-based immunochemical assays [21]. The C-ARF is the principal mechanism of the acoustic tweezers that are capable of separating, enriching, and patterning bioparticles in complex solutions [22], [23]. A recent review of the acoustic-tweezer technology and its applications in biology and medicine, including isolation of circulating biomarkers, and single-cell analysis, are presented in [23]. There are several applications of radiation force in microfluidics and biotechnology [11]. In various biotechnological applications, the diffusion rate in microvolumes of liquids is the main factor limiting the efficiency of the process of interest. A new technique, called the "swept-frequency method" [20], based on the use of radiation force in the standing acoustic wave for microstirring and mixing liquids may provide a solution to this problem. Adapting these techniques to the needs of current biotechnology, microfluidics, and nanotechnology often deals with microliter and submicroliter volumes of liquids. There are numerous biotechnological applications where diffusion is the main factor limiting the rate and efficiency of the process, such as in microarrays, which are widely used for the identification of proteins, oligonucleotides, and other biologically important molecules. Microarray analysis became the basis for the recent advances in high-throughput technologies for studying genes and their functions. One of the drawbacks of a microarray analysis is the long testing time, which could be in the range of hours. Effective stirring of the sample tested by the microarray analysis may reduce diffusion limitation and may significantly improve the performance of the method. Such stirring can be achieved by adding a small amount of microparticles to the test sample and moving these particles by the radiation force of a standing acoustic wave. The theoretical basis of this stirring technique, named the "swept-frequency standing wave" method, is described in detail in [20]. By changing the frequency of the driving signal applied to the transducer of a resonator, various harmonics of the standing wave are generated, urging microparticles to jump from one nodal pattern to another. This method of microstirring was implemented in the system for ultrasound-assisted immuno-agglutination test for HIV detection [76]. Swept-frequency standing wave stirring helped to destroy nonspecifically bound aggregate, thus improving the sensitivity of the HIV detection method by nearly two orders of magnitude. Some of the other applications and the swept-frequency tools are described in [77].

D. Mechanism D

The ARF based on mechanism (D), let it be called D-ARF, results from the variation in acoustic energy density due to gradients of compressional wave speeds and mass densities in the medium [31], [78]. Similar to B-ARF, it also is not related to the dissipation of energy. Consider an undamped plane wave $p^{\mathrm{IN}}(t - x/c_1)$ incident on the interface between two media. This wave propagates from a medium where the speed of sound and density are c_1, ρ_1 to the medium with parameters c_2, ρ_2. The acoustic pressures on the boundary are equal on both sides. On the contrary, the radiation forces are different. The difference between these forces is

$$\langle F_x^{\mathrm{NL}} \rangle_1 - \langle F_x^{\mathrm{NL}} \rangle_2 = S\left(\frac{1}{c_1^2 \rho_1} - \frac{1}{c_2^2 \rho_2}\right)\langle p^2 \rangle \tag{12}$$

where $p = p^{\mathrm{IN}}$ is as defined above. The resulting force can have different signs, which will lead to either pushing the boundary from the ultrasonic source or pulling toward it [78]. This possibility of changing the direction of force was first demonstrated in the experiment of Hertz and Mende [7].

The effects of this D-ARF are most pronounced in sonication of the medium by short ultrasonic pulses with durations on the order of microseconds. The D-ARF is generated locally at the boundaries between tissue structures and the contribution of D-ARF could be pronounced in the case of short excitation pulses in the microsecond range, as it follows from available experimental data [78]. At longer ultrasound exposures in the range of milliseconds and longer, which are typically used in many acoustic imaging technologies, the contribution of D-ARF becomes negligible relative to A-ARF because of great absorption of ultrasound in biological tissues. The pushing or pulling effects of D-ARF will depend on the sign of the gradient of the energy density of the boundary between adjacent media. Under the action of the radiation force (12), the interface between the adjacent media bends until the radiation force is compensated by the restoring elastic force. This force tends to smooth out the convexity of the boundary and return it to its original position. The time dependence of the displacement is determined by the envelope of the ultrasonic pulse $P_0(t)$ and, as the calculation shows, is

$$X(t) = \frac{\gamma}{G}\langle F_x^{\mathrm{NL}} \rangle \sim P_0^2(t). \tag{13}$$

This force is inversely proportional to the shear elasticity G of the soft tissue. Formula (13) is derived as a solution to a simple problem in the theory of elasticity, namely, to the problem of the dynamic deformation of an elastic half-space, to the boundary of which a time-varying radiation force is applied. This force is created by an acoustic wave beam bounded in a cross-section. Here γ is a form factor that depends on the structure of the acoustic beam and its cross-sectional area. Formula (13) has a transparent physical meaning. The greater the radiation force $\langle F_x^{\mathrm{NL}} \rangle$, and the lower the shear elasticity G of the medium, the greater the deflection $X(t)$ of the boundary. If instead of a soft solid we have an interface between two liquids, like in the experiment of Hertz and Mende, the formula (13), instead of shear elasticity G, will contain surface tension and gravity force due to the difference in the density of two liquid media.

It is seen that with a decrease in the envelope duration, the boundary displacement velocity can increase, as the velocity is proportional to the time derivative of $X(t)$, or of the square of the envelope of the ultrasound pulse, $P_0^2(t)$. Thus, the Doppler frequency shift of the recorded signal will also increase. This makes it possible to perform a local (within the cross-section of the focused beam) measurement of module G.

The main difference between B-ARF and D-ARF is that B-ARF may produce only a pushing effect on tissue, while D-ARF can be both pushing and pulling depending on the sign of the gradient of the energy density of the propagating wave [31]. The main similarity of B-ARF and D-ARF is that both are generated locally at the boundary between tissue structures and are "nondissipative," that is, they do not depend on the attenuation of ultrasound. On the contrary, A-ARF is a bulk volumetric effect, depending on both ultrasound attenuation coefficient of the tissue and the duration of the ultrasonic pulse. The longer the pulse, the larger the volume of tissue affected by ultrasound and greater is A-ARF. But with decreasing the pulse duration, the contribution of A-ARF becomes negligible relative to B-ARF and D-ARF. The contribution of B-ARF relative to D-ARF, analyzed in [78] using theory of D-ARF developed by Beyer [79] is shown to be on the order of a few percent. For example, it is estimated that the contributions of B-ARF relative to the D-ARF acting on the interface between blood and liver and between blood and brain are 1.7% and 4.2% correspondingly. In [78], it was shown that in sonicating the tissues mimicking medium by short ultrasonic pulses in the microsecond's range, where the contribution of A-ARF is negligible, D-ARF provides the main contribution to net radiation force. Therefore, we may hypothesize that D-ARF is a significant phenomenon in conventional ultrasound exams where microsecond scale pulses are used. However, there are no studies related to this phenomenon and it could be an important subject for future research related to the physics of ultrasonic imaging.

1) Biomedical Applications: As shown in [78], the D-ARF can be used for remote measurement of shear elasticity of soft tissue samples. In a broader spectrum, the D-ARF mechanism has not been used extensively in biomedical applications, as the contribution of D-ARF becomes negligible compared to A-ARF in typical biomedical ultrasound systems.

III. Selected Ideas on Future Biomedical Applications

In addition to the well-established applications mentioned above, the ARF has considerable potential in numerous other biomedical areas.

Despite the fact that ARF-based imaging modalities have advanced significantly in recent years (for example, advances in ARF-based elastography are described in [24]), there are still some poorly explored areas in this field. The ability of SWEI to quantitatively assess tissue's multiple parameters, such as viscosity, elasticity, and anisotropy, was never fully implemented in the current commercially available elastography devices to design a composite multidimensional tissue characterization tool. Such multidimensional parameters may serve as a new powerful biomarker for differentiating masses in tissue.

Another potential application of ARF is the estimation of nonlinear elasticity. To date, different approaches have been proposed for this application. A method presented in [80] uses static elastography and SWE together to derive the nonlinear shear modulus utilizing the acoustoelasticity principles. Another approach, named C-elastography, estimates the local third-order modulus of elasticity at the focus of the ultrasound beam. The theory and early results of this approach can be found in [81] and [82]. The potential application of ARF for the assessment of the skeletal system described in [11] needs to be further developed. The application is based on remotely generating different modes of acoustical waves in bones using radiation force and evaluating the propagation parameters of the waves sensitive to both mechanical and structural features of the bones [83]. This approach would greatly increase the potential of bone ultrasonometry for osteoporosis assessment [84] and, especially for applications related to neonatology. The development of methods for assessment of the skeletal system in newborns and infants, where conventional bone ultrasonometry is inapplicable and X-ray densitometry is restricted in its application, is extremely important. The problem is especially vital because of the growing incidences of osteopenia of prematurity, which decreased bone mass and density in premature and low-birth-weight infants to assess newborn bone growth and ossification [85], [86].

As mentioned above, the D-ARF has never been employed in biomedical applications. However, we hypothesize that there is a possibility of developing new elastometric and elastographic technologies based on the use of D-ARF induced by the microsecond scale, high-intensity ultrasonic pulses. The pattern of deformations induced by D-ARF has additional information relative to that provided by conventional elasticity imaging. Tissue structures could be potentially visualized in terms of variation in acoustic energy density due to the gradients of acoustic properties at the boundaries between adjacent tissue structures. The contribution of A-ARF can be neglected in the case of short excitation pulses because D-ARF is generated locally at the boundaries between tissue structures, in contrast to A-ARF, which is a bulk volumetric effect. However, the main problem is the detectability of nanometer-scale motion induced by microsecond range ultrasound pulses, and it may seem impossible to make use of D-ARF for imaging and elastographic applications. However, there are preliminary experimental data demonstrating the possibility of using a continuous wave Doppler to detect the motion induced by the D-ARF [78].

Imaging application of D-ARF might be possible with the use of principles of ultrafast ultrasound, an emerging modality in medical imaging [87], [88]. Ultrafast ultrasound imaging is achieved by transmitting an unfocused wave, recording the resulting backscattered echoes and performing digital parallel beamforming of the echoes to reconstruct the ultrasonic image from a single transmission. Building an image is mainly limited by the time required for a wave to make a two-way travel, which is less than 0.1 ms for the imaging depth of up to 7 cm. It should be noted that D-ARF detection by ultrafast ultrasound may be inhibited by the loss in SNR and spatial resolution due to high frame rate. Several ultrafast imaging technologies have emerged in the last decade, including ultrafast Doppler imaging [88]. We hypothesize that elastographic application of D-ARF, which we may call Ultrafast Elastography, should be based on visualizing the pattern of Doppler signals induced by an ultrasonic pulse propagating through a composite medium containing numerous interfaces between structures differing in ultrasound velocity. The pattern of Doppler signals will contain information on the map of tissue elasticity. To make that map quantitative, additional estimates of ultrasonic parameters of tissues will be needed. The feasibility of the proposed ultrafast elastography will depend on the sensitivity of the Doppler imaging. Based on our experimental data [75], the necessary sensitivity should be on the order of mm/s, which is close to the range achieved in the application of ultrafast Doppler imaging to blood flow speed measured in the brain [88], [89]. There is a chance that the use of D-ARF for ultrasound imaging and tissue characterization could serve as a basis for a new mode of elastography.

IV. Conclusion

This article describes four mechanisms for the generation of ARF in tissue-like media. Examples of biomedical applications are presented. Although ARF has been successfully used in a wide range of biomedical applications, particularly in medical imaging, there are still many application areas that remain to be explored.

Acknowledgment

The authors would like to thank Ms. Shaheeda A. Adusei (M.S.), Ms. Yinong Wang (M.S.), and Dr. Juanjuan Gu for formatting this manuscript.

References

[1] A. P. Sarvazyan, O. V. Rudenko, and W. L. Nyborg, "Biomedical applications of radiation force of ultrasound: Historical roots and physical basis," *Ultrasound Med. Biol.*, vol. 36, no. 9, pp. 1379–1394, Sep. 2010.

[2] M. Faraday, "XVII. On a peculiar class of acoustical figures; and on certain forms assumed by groups of particles upon vibrating elastic surfaces," *Philos. Trans. Roy. Soc. London*, vol. 121, pp. 299–340, Dec. 1831.

[3] A. Kundt and O. Lehmann, "Ueber longitudinale schwingungen und klangfiguren in cylindrischen Flüssigkeitssäulen," *Ann. Phys. Chem.*, vol. 229, no. 9, pp. 1–12, 1874.

[4] L. Rayleigh, "XXXIV. On the pressure of vibrations," *London, Edinburgh, Dublin Phil. Mag. J. Sci.*, vol. 3, no. 15, pp. 338–346, Mar. 1902.

[5] V. F. K. Bjerknes, *Die Kraftfelder, Braunschweig*. Berlin, Germany: Vieweg Sohn, 1909.

[6] R. W. Wood and A. L. Loomis, "XXXVIII. The physical and biological effects of high-frequency sound-waves of great intensity," *Lond. Edinb. Dubl. Phil. Mag. J. Sci.*, vol. 4, no. 22, pp. 417–436, Sep. 1927.

[7] G. Hertz and H. Mende, "Der schallstrahlungsdruck in flüssigkeiten," *Zeitschrift Phys.*, vol. 114, nos. 5–6, pp. 354–367, May 1939.

[8] P. Biquard, "Les ondes ultra-sonores," *Rev. Acoust.*, vol. 1, pp. 93–109, Oct. 932.

[9] W. L. Nyborg, "Mechanisms for nonthermal effects of sound," *J. Acoust. Soc. Amer.*, vol. 44, no. 5, pp. 1302–1309, Nov. 1968.

[10] W. L. Nyborg, "Physical principles of ultrasound," in *Ultrasound: Its Applications in Medicine and Biology*, F. J. Fry, Ed. Amsterdam, The Netherlands: Elsevier, 1978, pp. 1–75.

[11] A. Sarvazyan, "Diversity of biomedical applications of acoustic radiation force," *Ultrasonics*, vol. 50, no. 2, pp. 230–234, Feb. 2010.

[12] K. Nightingale, "Acoustic radiation force impulse (ARFI) imaging: A review," *Current. Med. Imag. Rev.*, vol. 7, no. 4, pp. 328–339, Nov. 2011.

[13] K. Nightingale *et al.*, "Acoustic radiation force impulse imaging: *In vivo* demonstration of clinical feasibility," *Ultrasound Med. Biol.*, vol. 28, no. 2, pp. 227–235, Feb. 2002.

[14] L. P. Gor'kov, "On the forces acting on a small particle in an acoustical field in an ideal fluid," *Sov. Phys.-Dokl.*, vol. 6, pp. 773–775, 1962.

[15] W. T. Coakley, J. J. Hawkes, M. A. Sobanski, C. M. Cousins, and J. Spengler, "Analytical scale ultrasonic standing wave manipulation of cells and microparticles," *Ultrasonics*, vol. 38, nos. 1–8, pp. 638–641, Mar. 2000.

[16] A. Haake *et al.*, "Manipulation of cells using an ultrasonic pressure field," *Ultrasound Med. Biol.*, vol. 31, no. 6, pp. 857–864, Jun. 2005.

[17] H. Bruus, "Acoustofluidics: Theory and simulation of streaming and radiation forces at ultrasound resonances in microfluidic devices," *J. Acoust. Soc. Amer.*, vol. 125, no. 4, p. 2592, Apr. 2009.

[18] J. Hultström *et al.*, "Proliferation and viability of adherent cells manipulated by standing-wave ultrasound in a microfluidic chip," *Ultrasound Med. Biol.*, vol. 33, no. 1, pp. 145–151, Jan. 2007.

[19] W. T. Coakley, D. W. Bardsley, M. A. Grundy, F. Zamani, and D. J. Clarke, "Cell manipulation in ultrasonic standing wave fields," *J. Chem. Technol. Biotechnol.*, vol. 44, no. 1, pp. 43–62, Apr. 2007.

[20] A. Sarvazyan and L. Ostrovsky, "Stirring and mixing of liquids using acoustic radiation force," *J. Acoust. Soc. Amer.*, vol. 125, no. 6, pp. 3548–3554, Jun. 2009.

[21] M. Wiklund and H. M. Hertz, "Ultrasonic enhancement of bead-based bioaffinity assays," *Lab Chip*, vol. 6, no. 10, pp. 1279–1292, Oct. 2006.

[22] J. Lee and K. K. Shung, "Effect of ultrasonic attenuation on the feasibility of acoustic tweezers," *Ultrasound Med. Biol.*, vol. 32, no. 10, pp. 1575–1583, Oct. 2006.

[23] A. Ozcelik *et al.*, "Acoustic tweezers for the life sciences," *Nature Methods*, vol. 15, pp. 1021–1028, Nov. 2018.

[24] A. Sarvazyan, T. J. Hall, M. W. Urban, M. Fatemi, S. R. Aglyamov, and B. Garra, "Elasticity imaging-an emerging branch of medical imaging. An overview," *Current Meds. Imag. Rev.*, vol. 7, no. 4, pp. 255–282, 2011.

[25] A. P. Sarvazyan *et al.*, "Shear wave elasticity imaging: A new ultrasonic technology of medical diagnostics," *Ultrasound Med. Biol.*, vol. 24, no. 9, pp. 1419–1435, Nov. 1998.

[26] P. N. T. Wells, *Biomedical Ultrasonics*. New York, NY, USA: Academic, 1977.

[27] L. D. Landau, and L. P. Pitaevskii, *Theory of Elasticity*, 3rd ed. New York, YN, USA: Pergamon Press, 1986.

[28] L. D. Landau, and E. M. Lifshitz, *Fluid Mechanics*, 2ed ed. New York, YN, USA: Pergamon Press, 1987.

[29] O. V. Rudenko, "Giant nonlinearities in structurally inhomogeneous media and the fundamentals of nonlinear acoustic diagnostic techniques," *Phys-Usp*, vol. 49, no. 1, p. 69, 2006.

[30] O. V. Rudenko, "Nonlinear waves: Some biomedical applications," *Phys-Usp*, vol. 50, no. 4, p. 359, 2007.

[31] L. Ostrovsky *et al.*, "Non-dissipative mechanisms of radiation force and shear wave generation," *J. Acoust. Soc. Amer.*, vol. 118, no. 3, p. 2006, Sep. 2005.

[32] J. Bercoff, M. Tanter, and M. Fink, "Supersonic shear imaging: A new technique for soft tissue elasticity mapping," *IEEE Trans. Ultrason., Ferroelectr., Freq. Control*, vol. 51, no. 4, pp. 396–409, Apr. 2004.

[33] E. E. Konofagou and K. Hynynen, "Localized harmonic motion imaging: Theory, simulations and experiments," *Ultrasound Med. Biol.*, vol. 29, no. 10, pp. 1405–1413, Oct. 2003.

[34] Z. Hah, C. Hazard, Y. T. Cho, D. Rubens, and K. Parker, "Crawling waves from radiation force excitation," *Ultrason. Imag.*, vol. 32, no. 3, pp. 177–189, Jul. 2010.

[35] S. Chen *et al.*, "Shearwave dispersion ultrasound vibrometry (SDUV) for measuring tissue elasticity and viscosity," *IEEE Trans. Ultrason., Ferroelectr., Freq. Control*, vol. 56, no. 1, pp. 55–62, Jan. 2009.

[36] I. Z. Nenadic *et al.*, "Lamb wave dispersion ultrasound vibrometry (LDUV) method for quantifying mechanical properties of viscoelastic solids," *Phys. Med. Biol.*, vol. 56, no. 7, p. 2245, 2011.

[37] I. Z. Nenadic *et al.*, "Attenuation measuring ultrasound shearwave elastography and *in vivo* application in post-transplant liver patients," *Phys. Med. Biol.*, vol. 62, no. 2, p. 484, 2016.

[38] C. Amador *et al.*, "Loss tangent and complex modulus estimated by acoustic radiation force creep and shear wave dispersion," *Phys. Med. Biol.*, vol. 57, no. 5, p. 1263, 2012.

[39] P. Kijanka and M. W. Urban, "Local phase velocity based imaging: A new technique used for ultrasound shear wave elastography," *IEEE Trans. Med. Imag.*, vol. 38, no. 4, pp. 894–908, Apr. 2019.

[40] M. R. Selzo and C. M. Gallippi, "Viscoelastic response (VisR) imaging for assessment of viscoelasticity in voigt materials," *IEEE Trans. Ultrason., Ferroelectr., Freq. Control*, vol. 60, no. 12, pp. 2488–2500, Dec. 2013.

[41] T. Deffieux, G. Montaldo, M. Tanter, and M. Fink, "Shear wave spectroscopy for *in vivo* quantification of human soft tissues visco-elasticity," *IEEE Trans. Med. Imag.*, vol. 28, no. 3, pp. 313–322, Mar. 2009.

[42] C. A. Trutna, N. C. Rouze, M. L. Palmeri, and K. R. Nightingale, "Measurement of viscoelastic material model parameters using fractional derivative group shear wave speeds in simulation and phantom data," *IEEE Trans. Ultrason., Ferroelectr., Freq. Control*, vol. 67, no. 2, pp. 286–295, Feb. 2020.

[43] K. J. Parker, J. Ormachea, F. Zvietcovich, and B. Castaneda, "Reverberant shear wave fields and estimation of tissue properties," *Phys. Med. Biol.*, vol. 62, no. 3, p. 1046, 2017.

[44] P. Kijanka and M. W. Urban, "Two-point frequency shift method for shear wave attenuation measurement," *IEEE Trans. Ultrason., Ferroelectr., Freq. Control*, vol. 67, no. 3, pp. 483–496, Mar. 2020.

[45] S. McAleavey, M. Menon, and E. Elegbe, "Shear modulus imaging with spatially-modulated ultrasound radiation force," *Ultrason. Imag.*, vol. 31, no. 4, pp. 217–234, 2009.

[46] R. M. Sigrist, J. Liau, A. El Kaffas, M. C. Chammas, and J. K. Willmann, "Ultrasound elastography: Review of techniques and clinical applications," *Theranostics*, vol. 7, no. 5, pp. 1303–1329, 2017.

[47] R. G. Barr *et al.*, "WFUMB guidelines and recommendations for clinical use of ultrasound elastography: Part 2: Breast," *Ultrasound Med. Biol.*, vol. 41, no. 5, pp. 1148–1160, 2015.

[48] G. Ferraioli *et al.*, "WFUMB guidelines and recommendations for clinical use of ultrasound elastography: Part 3: Liver," *Ultrasound Med. Biol.*, vol. 41, no. 5, pp. 1161–1179, 2015.

[49] D. Cosgrove *et al.*, "WFUMB guidelines and recommendations on the clinical use of ultrasound elastography: Part 4. Thyroid," *Ultrasound Med. Biol.*, vol. 43, no. 1, pp. 4–26, 2017.

[50] R. G. Barr *et al.*, "WFUMB guidelines and recommendations on the clinical use of ultrasound elastography: Part 5. Prostate," *Ultrasound Med. Biol.*, vol. 43, no. 1, pp. 27–48, 2017.

[51] C. Dietrich *et al.*, "EFSUMB guidelines and recommendations on the clinical use of liver ultrasound elastography, update 2017 (Long Version)," *Ultraschall Med. Eur. J. Ultrasound*, vol. 38, no. 4, p. e48, Aug. 2017.

[52] I. Nenadic *et al.*, "Noninvasive evaluation of bladder wall mechanical properties as a function of filling volume: Potential application in bladder compliance assessment," *PLoS ONE*, vol. 11, no. 6, Jun. 2016, Art. no. e0157818.

[53] M. Bayat *et al.*, "Correlation of ultrasound bladder vibrometry assessment of bladder compliance with urodynamic study results," *PLoS ONE*, vol. 12, no. 6, Jun. 2017, Art. no. e0179598.

[54] X. Zhang, D. A. Husmann, L. A. Mynderse, A. Alizad, and M. Fatemi, "Non-invasive assessment of urinary bladder compliance using ultrasound: First validation study based on clinical urodynamic study," *Ann. Transl. Med.*, vol. 9, no. 7, p. 547, Apr. 2021.

[55] X. Zhang, R. R. Kinnick, M. Fatemi, and J. F. Greenleaf, "Noninvasive method for estimation of complex elastic modulus of arterial vessels," *IEEE Trans. Ultrason., Ferroelectr., Freq. Control*, vol. 52, no. 4, pp. 642–652, Apr. 2005.

[56] M. Bernal, I. Nenadic, M. W. Urban, and J. F. Greenleaf, "Material property estimation for tubes and arteries using ultrasound radiation force and analysis of propagating modes," *J. Acoust. Soc. Amer.*, vol. 129, no. 3, pp. 1344–1354, Mar. 2011.

[57] M. Fatemi and J. F. Greenleaf, "Vibro-acoustography: An imaging modality based on ultrasound-stimulated acoustic emission," *Proc. Nat. Acad. Sci. USA*, vol. 96, no. 12, pp. 6603–6608, 1999.

[58] M. W. Urban, A. Alizad, W. Aquino, J. F. Greenleaf, and M. Fatemi, "A review of vibro-acoustography and its applications in medicine," *Current Med. Imag.*, vol. 7, no. 4, pp. 350–359, 2011.

[59] M. Fatemi and J. F. Greenleaf, "Ultrasound-stimulated vibro-acoustic spectrography," *Science*, vol. 280, no. 5360, pp. 82–85, Apr. 1998.

[60] T. Hasegawa, T. Kido, C. Matsuoka, and T. Iizuka, "A general theory of Rayleigh and Langevin radiation pressures," *Acoust. Sci. Technol.*, vol. 21, no. 3, pp. 145–152, 2000.

[61] R. T. Beyer, "Radiation pressure-the history of a mislabeled tensor," *J. Acoust. Soc. Amer.*, vol. 63, no. 4, pp. 1025–1030, Apr. 1978.

[62] Z. Gol'dberg, "Acoustic radiation pressure," in *High Intensity Ultrasonic Fields*, L. D. Rozenberg, Ed. Boston, MA, USA: Springer, 1971. pp. 73–113.

[63] M. Fatemi and J. F. Greenleaf, "Probing the dynamics of tissue at low frequencies with the radiation force of ultrasound," *Phys. Med. Biol.*, vol. 45, no. 6, p. 1449, Jun. 2000.

[64] A. Alizad *et al.*, "Breast vibro-acoustography: Initial experience in benign lesions," *BMC Med. Imag.*, vol. 14, no. 1, p. 40, Dec. 2014.

[65] M. Mehrmohammadi *et al.*, "Preliminary *in vivo* breast vibro-acoustography results with a Quasi-2-D array transducer: A step forward toward clinical applications," *Ultrasound Med. Biol.*, vol. 40, no. 12, pp. 2819–2829, Dec. 2014.

[66] A. Alizad *et al.*, "Breast vibro-acoustography: Initial results show promise," *Breast Cancer Res.*, vol. 14, no. 5, Sep. 2012.

[67] A. Alizad *et al.*, "*In vivo* thyroid vibro-acoustography: A pilot study," *BMC Med. Imag.*, vol. 13, no. 1, p. 12, Mar. 2013.

[68] F. G. Mitri *et al.*, "Prostate cryotherapy monitoring using vibroacoustography: Preliminary results of anEx VivoStudy and technical feasibility," *IEEE Trans. Biomed. Eng.*, vol. 55, no. 11, pp. 2584–2592, Nov. 2008.

[69] F. G. Mitri *et al.*, "Vibro-acoustography imaging of permanent prostate brachytherapy seeds in an excised human prostate–preliminary results and technical feasibility," *Ultrasonics*, vol. 49, no. 3, pp. 389–394, Mar. 2009.

[70] M. Mehrmohammadi, A. Alizad, R. R. Kinnick, B. J. Davis, and M. Fatemi, "Feasibility of vibro-acoustography with a quasi-2D ultrasound array transducer for detection and localizing of permanent prostate brachytherapy seeds: A pilot ex vivo study," *Med. Phys.*, vol. 41, no. 9, Sep. 2014, Art. no. 092902.

[71] F. G. Mitri and R. R. Kinnick, "Vibroacoustography imaging of kidney stones *in vitro*," *IEEE Trans. Biomed. Eng.*, vol. 59, no. 1, pp. 248–254, Jan. 2012.

[72] C. Pislaru *et al.*, "*In vivo* vibroacoustography of large peripheral arteries," *Invest. Radiol.*, vol. 43, no. 4, pp. 243–252, Apr. 2008.

[73] A. Alizad and M. Fatemi, "Vibro-acoustography and its medical applications," *Ultrasound Elastography for Biomedical Applications and Medicine*. Hoboken, NJ, USA: Wiley, 2018, pp. 250–263.

[74] A. Shah *et al.*, "Novel ultrasound method to reposition kidney stones," *Urol. Res.*, vol. 38, no. 6, pp. 491–495, Dec. 2010.

[75] O. V. Rudenko, A. P. Sarvazyan, and S. Y. Emelianov, "Acoustic radiation force and streaming induced by focused nonlinear ultrasound in a dissipative medium," *J. Acoust. Soc. Amer.*, vol. 99, no. 5, pp. 2791–2798, May 1996.

[76] S. Bystryak and N. Ossina, "A rapid ultrasound particle agglutination method for HIV antibody detection: Comparison with conventional rapid HIV tests," *J. Virol. Methods*, vol. 249, pp. 38–47, Nov. 2017.

[77] A. P. Sarvazyan, "Apparatus for ultrasonic stirring of liquids in small volumes," U.S. Patent 7980752 B2, Jul. 19, 2011.

[78] A. Sarvazyan and S. Tsyuryupa, "Potential biomedical applications of non-dissipative acoustic radiation force," in *Proc. OMA*, Salt Lake City, UT, USA, 2016, Art. no. 020002.

[79] R. T. Beyer, *Nonlinear acoustics: US Department of Defense*. Washington, DC, USA: Naval Sea Systems Command, 1974, p. 234.

[80] H. Latorre-Ossa, J.-L. Gennisson, E. De Brosses, and M. Tanter, "Quantitative imaging of nonlinear shear modulus by combining static elastography and shear wave elastography," *IEEE Trans. Ultrason., Ferroelectr., Freq. Control*, vol. 59, no. 4, pp. 833–839, Apr. 2012.

[81] D. P. Shahraki *et al.*, "C-elastography: *In vitro* feasibility phantom study," *Ultrasound Med. Biol.*, vol. 46, no. 7, pp. 1738–1754, Jul. 2020.

[82] B. B. Guzina, E. V. Dontsov, M. W. Urban, and M. Fatemi, "The 'sixth sense' of ultrasound: Probing nonlinear elasticity with acoustic radiation force," *Phys. Med. Biol.*, vol. 60, no. 9, pp. 3775–3794, May 2015.

[83] S. Ghavami *et al.*, "Ultrasound radiation force for the assessment of bone fracture healing in children: An *in vivo* pilot study," *Sensors*, vol. 19, no. 4, p. 955, Feb. 2019.

[84] S. Ghavami *et al.*, "Pulsed vibro-acoustic method for assessment of osteoporosis & osteopenia: A feasibility study on human subjects," *J. Mech. Behav. Biomed. Mater.*, vol. 97, pp. 187–197, Sep. 2019.

[85] M. F. Faienza *et al.*, "Metabolic bone disease of prematurity: Diagnosis and management," *Frontiers Pediatrics*, vol. 7, p. 143, Apr. 2019.

[86] Y. Fatemi, "Introducing a new ultrasound-based technique for quantitative assessment of infant bone," in *Proc. AAP*, New Orleans, LA, USA, Oct. 2012, p. 17500.

[87] M. Tanter and M. Fink, "Ultrafast imaging in biomedical ultrasound," *IEEE Trans. Ultrason., Ferroelectr., Freq. Control*, vol. 61, no. 1, pp. 102–119, Jan. 2014.

[88] J. Bercoff *et al.*, "Ultrafast compound Doppler imaging: Providing full blood flow characterization," *IEEE Trans. Ultrason., Ferroelectr., Freq. Control*, vol. 58, no. 1, pp. 134–147, Jan. 2011.

[89] J. Provost, C. Papadacci, C. Demene, J.-L. Gennisson, M. Tanter, and M. Pernot, "3-D ultrafast Doppler imaging applied to the noninvasive mapping of blood vessels *in vivo*," *IEEE Trans. Ultrason., Ferroelectr., Freq. Control*, vol. 62, no. 8, pp. 1467–1472, Aug. 2015.

Armen P. Sarvazyan received the M.S. degree in physics from Moscow State University, Moscow, Russia, in 1964, and the Ph.D. and D.Sc. degrees in biophysics from the Institute of Biophysics, Russian Academy of Sciences, Moscow, in 1969 and 1983, respectively.

In 1992, he emigrated to the USA and established the Laboratory for Acoustical Studies of Biochemical Systems, Rutgers University, New Brunswick, NJ, USA. In 1995, he founded the Artann Laboratories, Lambertville, NJ, USA, a research and development company, funded by the National Institute of Health (NIH), NASA, Department of Defens (DoD), and Bill and Melinda Gates Foundation, developing biomechanical and ultrasonic technologies and instrumentation for laboratory and clinical applications. He has developed new modalities of medical imaging: tactile imaging and shear wave elastography. He holds more than 100 international patents on ultrasonic and biomechanical technologies and is the author or a coauthor of more than 200 research articles. His research interests cover wide diverse areas of medical ultrasound.

Dr. Sarvazyan is a fellow of the Acoustical Society of America and the International Professor Emeritus of the Department of Physics, Moscow State University. He received the Helmholtz-Rayleigh Interdisciplinary Silver Medal of the Acoustical Society of America in 2016. He was a recipient of the Pioneer Award of the History of Medical Ultrasound from the World Federation for Ultrasound in Medicine and Biology and American Institute of Ultrasound in Medicine, WA, USA, in 1988, and the 2021 IEEE Ultrasonics, Ferroelectrics, and Frequency Control (UFFC)-Ultrasonics Rayleigh Award for innovative and impactful contributions to the field of ultrasound tissue characterization and the invention of shear wave elastography.

Oleg V. Rudenko graduated from the Department of Physics, Lomonosov Moscow State University (MSU), Moscow, Russia, in 1971. He received the Ph.D. and D.Sc. degrees from the Department of Physics, Lomonosov MSU, in 1972 and 1981, respectively.

He is the author of 500 articles and 30 books. He conducted research in several branches of physics: mathematical physics, mechanics, acoustics, laser physics, earth sciences, underwater engineering, signal transmission, and ultrasonic medical technology. For many years, he headed the expert councils in physics of the Russian Foundation for Basic Research and the Higher Attestation Commission of Russia. He worked in Sweden for about 20 years. He is currently the Head of the Department of Acoustics, MSU, and the Chief Researcher of the Prokhorov Institute of General Physics and Schmidt Institute of the Physics of Earth, Russian Academy of Sciences (RAS), Moscow. He is also an Honored Professor of MSU and Lobachevsky State University of Nizhny Novgorod, Nizhny Novgorod, Russia. He was elected to RAS in 1997. He is a Full Member of the RAS (academician) since 2008, the only physicist-acoustician in Russia. He considers Nobel laureate Vitaly Ginzburg and academicians Rem Khokhlov and Alexander Dykhne as his scientific advisers and mentors.

Dr. Rudenko received the Union of Soviet Socialist Republics (USSR) State Prize in 1985 and the Russian State Prize in 1997, which are the highest scientific awards in Russia. He is the Editor-in-Chief of the *Acoustical Physics* and *Doklady Physics* and the Deputy Editor of the *Physics-Uspekhi*.

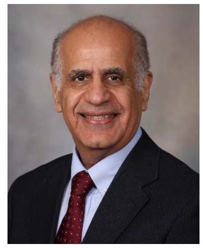

Mostafa Fatemi (Life Fellow, IEEE) received the Ph.D. degree in electrical engineering from Purdue University, West Lafayette, IN, USA, in 1979.

He joined Mayo in 1994, where he is currently a Professor of biomedical engineering with the Department of Physiology and Biomedical Engineering, Mayo Clinic College of Medicin and Science, Rochester, MN, USA. At the Mayo Clinic, he is also an Active Member of the Mayo Clinic Cancer Center and the Center for Clinical and Translational Science. His current research interests include developing novel ultrasonic methods for cancer imaging, microvasculature imaging, tissue viscoelasticity and nonlinear elasticity, and bladder function evaluation. His research program has been supported by major federal agencies, including the National Institute of Health (NIH), the National Science Foundation (NSF), and the Department of Defense, Congressionally Directed Medical Research Programs. He has published extensively on various biomedical applications of acoustic radiation force and he holds multiple patents in this area.

Dr. Fatemi is a fellow of the following institutions: the American Institute of Medical and Biological Engineering (AIMBE), the Acoustical Society of America (ASA), and the American Institute of Ultrasound in Medicine (AIUM). He was a recipient of the 2016 IEEE-Ultrasonics, Ferroelectrics, and Frequency Control (UFFC) Distinguished Lecturer Award.